



# Analysis of OCO-2 CO<sub>2</sub> flux inversion (MIP-2) using MIROC4-ACTM simulations

Suman Maity, Prabir K. Patra, Naveen Chandra, OCO2\_MIP and MIROC4-ACTM flux modellers

Research Institute for Global Change, JAMSTEC, Yokohama, Japan

## Background and method

Carbon dioxide (CO<sub>2</sub>) is the major anthropogenically produced greenhouse gas since the preindustrial era. A comprehensive understanding of the global carbon cycle is needed to analyze climate change and to anticipate the effect of future emission scenarios. Estimations of CO<sub>2</sub> emissions by sources and removals by sink over the globe by the top-down inverse modelling approach remained inconclusive due to the lack of adequate high-quality observations and due to the uncertainty in atmospheric transport.

Recently, using the Orbiting Carbon Observatory 2 (OCO2) observations of the total column CO<sub>2</sub> mixing ratio (XCO<sub>2</sub>), a Model Intercomparison Project (OCO2-MIP) was conducted by combining in situ CO<sub>2</sub> and OCO2 XCO<sub>2</sub> retrievals for the period 2015–2020 (Byrne et al., ESSDD, 2022; BB22). Although large differences between the estimated fluxes remained in the analyses of BB22, the evaluation with “independent” CO<sub>2</sub> data and assimilated model CO<sub>2</sub> fields do not provide clear indications of the model-model flux differences.

Here, we use the OCO2-MIP fluxes in comparison with our own inversions in JAMSTEC using the MIROC4 ACTM (Chandra et al., ACP, 2022; NC22). NC22 performed 16 ensemble inversions for testing dependence of inversion fluxes on the land and ocean prior fluxes and prior flux and data uncertainty under a single transport model framework, using in situ data only. All the inversions fluxes are run forward by MIROC4-ACTM to derive flux evaluation metric, with MIROC4-ACTM being a “perfect model” setting but bringing all OCO2-MIP fluxes on a common model transport.

## Model Description

MIROC4-ACTM is used here as a forward model.

**OCO2-MIP Fluxes considered (OCO2\_MIPv10)**

IS: In-situ data assimilated

LNLG: OCO2 Land nadir land glint data product assimilated

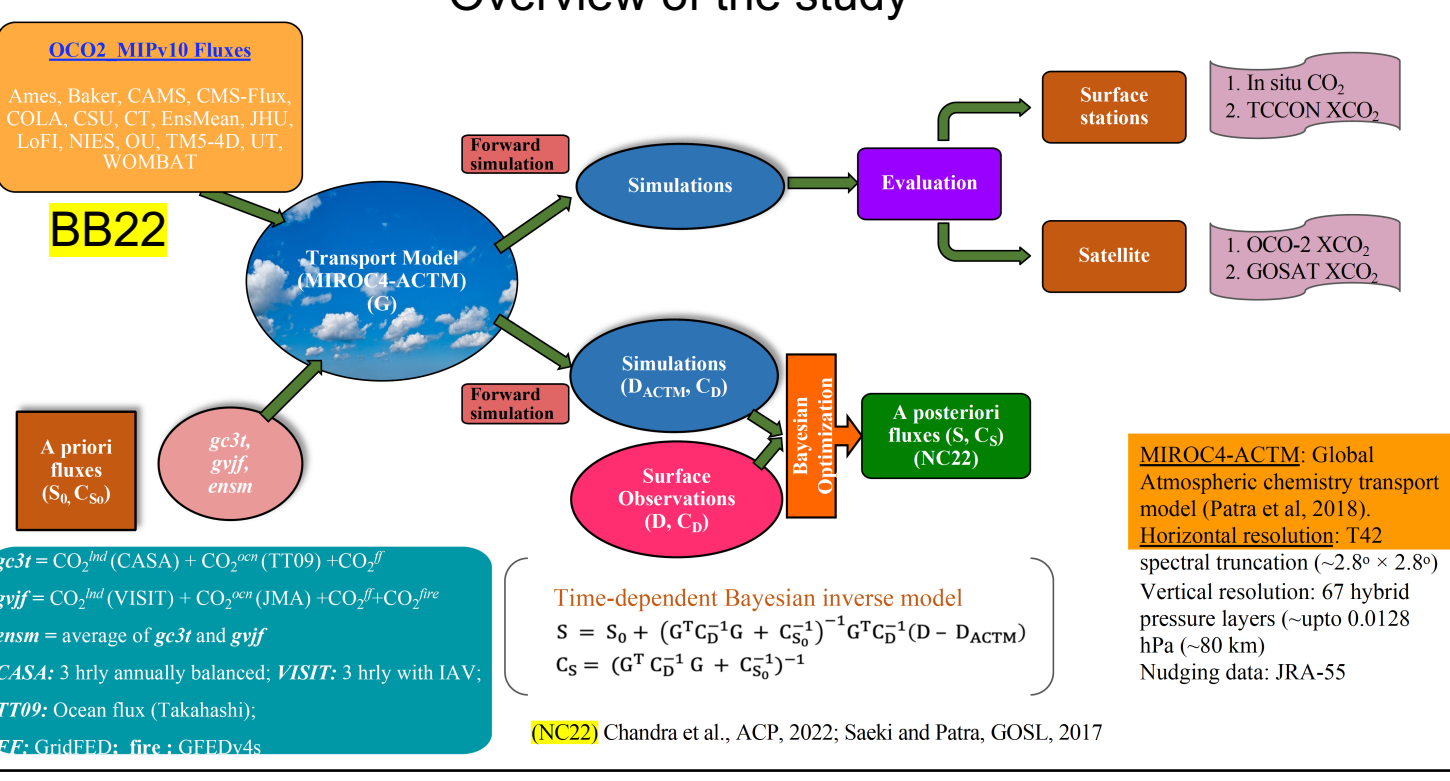
LNLGS: In-situ and OCO2 Land nadir land glint data assimilated

## Total combinations:

16 (15 OCO2-MIP and 1 MIROC4-ACTM data).

## Validation data:

TCCON, ObsPack, OCO2 and GOSAT datasets.



Simulated results are sampled, from hourly-average ACTM simulations, at the respective location and time of the observation for all comparisons

## Results

### Estimated 2015–2020 CO<sub>2</sub> fluxes

Figure 1 (below) compares CO<sub>2</sub> fluxes estimated by BB22 [multi-model mean (bar chart) and 1- $\sigma$  standard deviation (Error bar) in comparison with NC22 (symbols for 2 representative cases)] over (a) 15 land and (b) 11 oceanic regions. NC22 fluxes show good agreement with BB22 results, except for Tropical America, Europe, Russia, Southeast Asia.

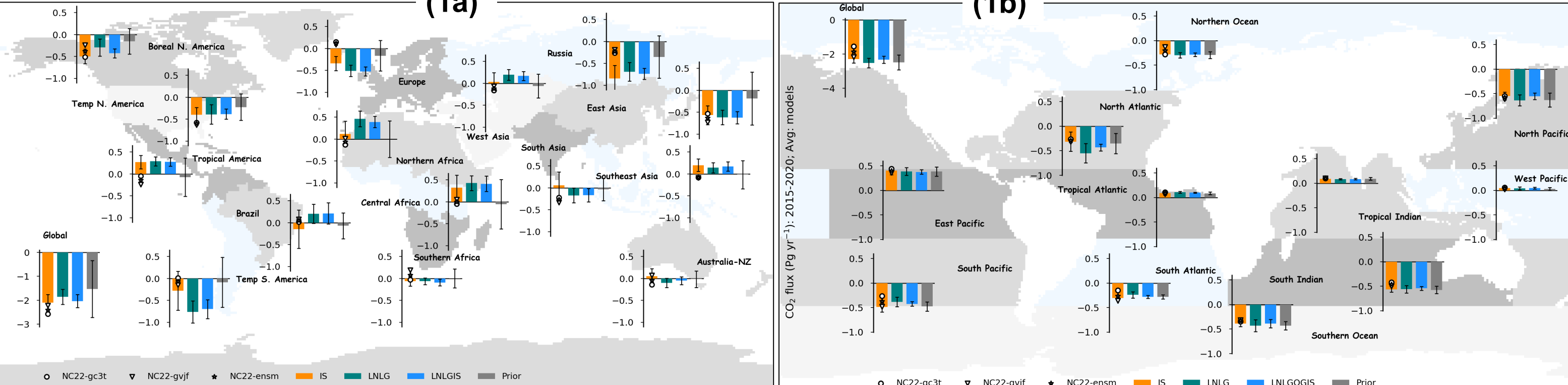


Figure 2 (below) shows net CO<sub>2</sub> fluxes. (a) annual mean over global land and global ocean (some of the models are not included in the analysis based on their anomalous behaviour, e.g., +ve or no IAV in ocean flux), (b) strong land vs. ocean flux dipole (2015–2020 mean values shown).

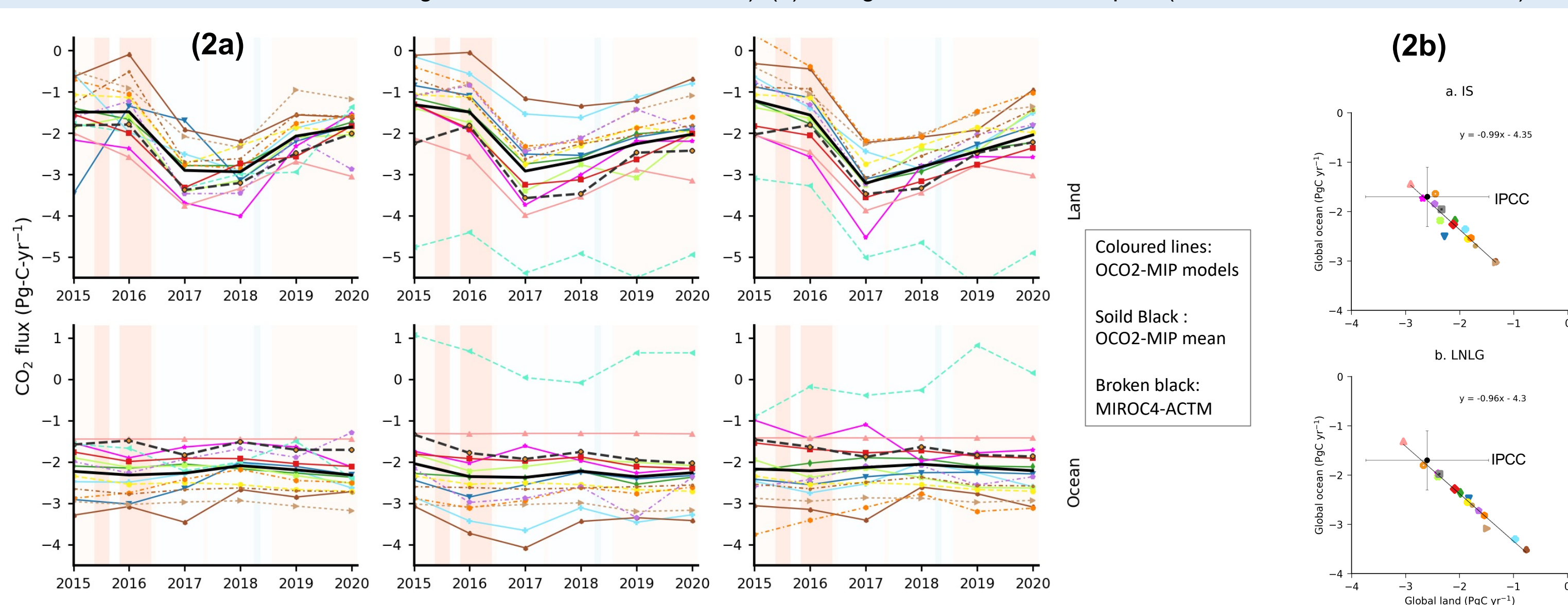
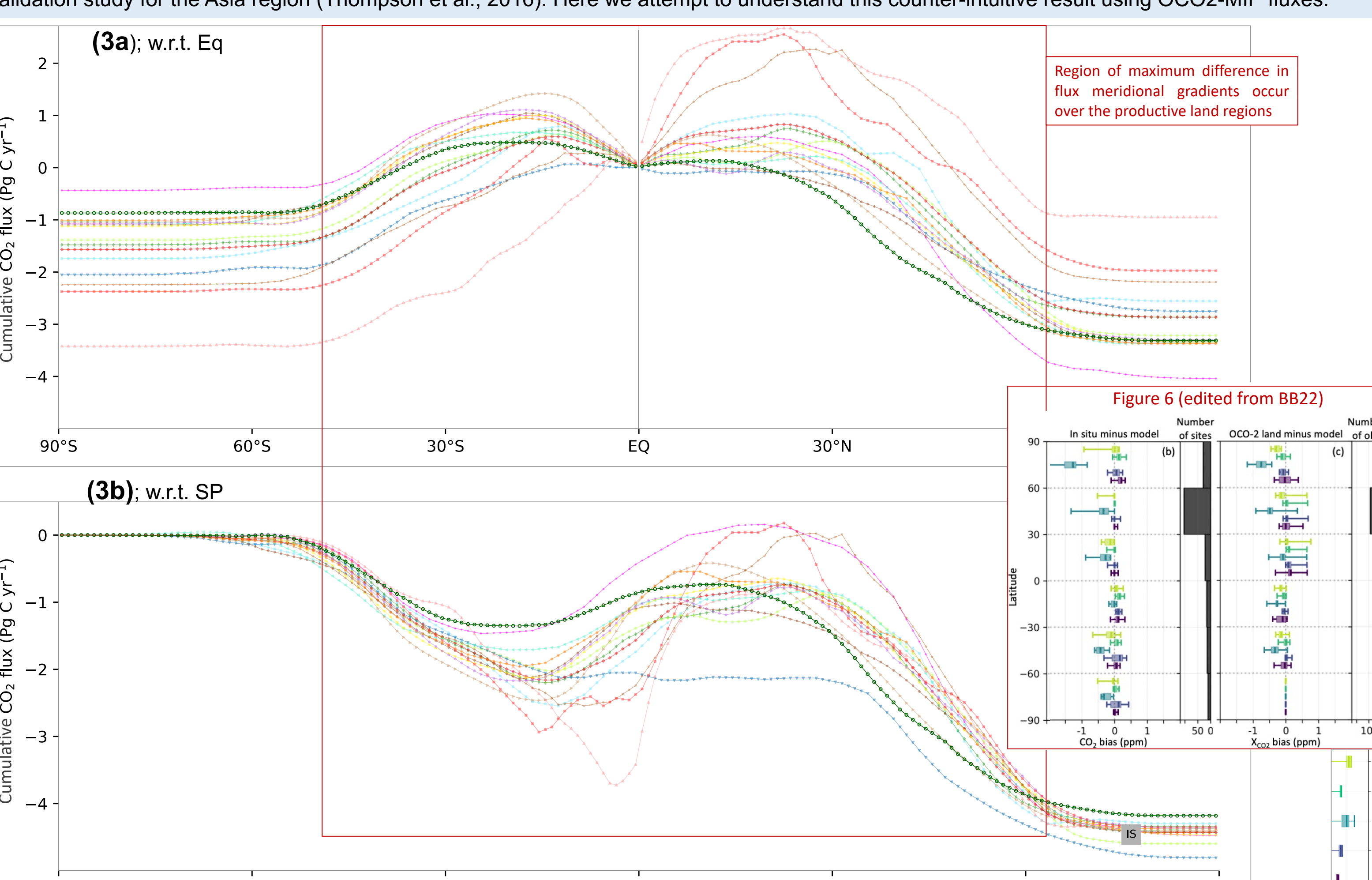


Figure 3 (below) shows meridional gradient of global total CO<sub>2</sub> flux. (a) cumulative poleward for both the hemispheres from Equator, (b) cumulative from South Pole to North Pole. The hemispheric total fluxes between models vary in the range of 2 to 4 PgC yr<sup>-1</sup> for the NH and 0.9 to 2.4 PgC yr<sup>-1</sup> for the SH. Global total flux are well constrained in the range of 4.2 to 4.6 PgC yr<sup>-1</sup>.

However, the large differences in flux meridional gradient (highlighted by red rectangle) did not show any meridional gradient for the observation – model concentration biases, as used for flux validation purpose in BB22 (inset Figure 6, edited). This situation also prevailed in earlier inversion flux validation study for the Asia region (Thompson et al., 2016). Here we attempt to understand this counter-intuitive result using OCO2-MIP fluxes.



## Results

Figure 4 (below) shows growth rate (GR) during 2015 – 2016 from In-situ, TCCON, GOSAT and OCO2 respectively. GR includes interannual variability and showing large standard deviations compare to BB22. Model GRs are generally in agreement with observations, a sanity check for ACTM simulations.

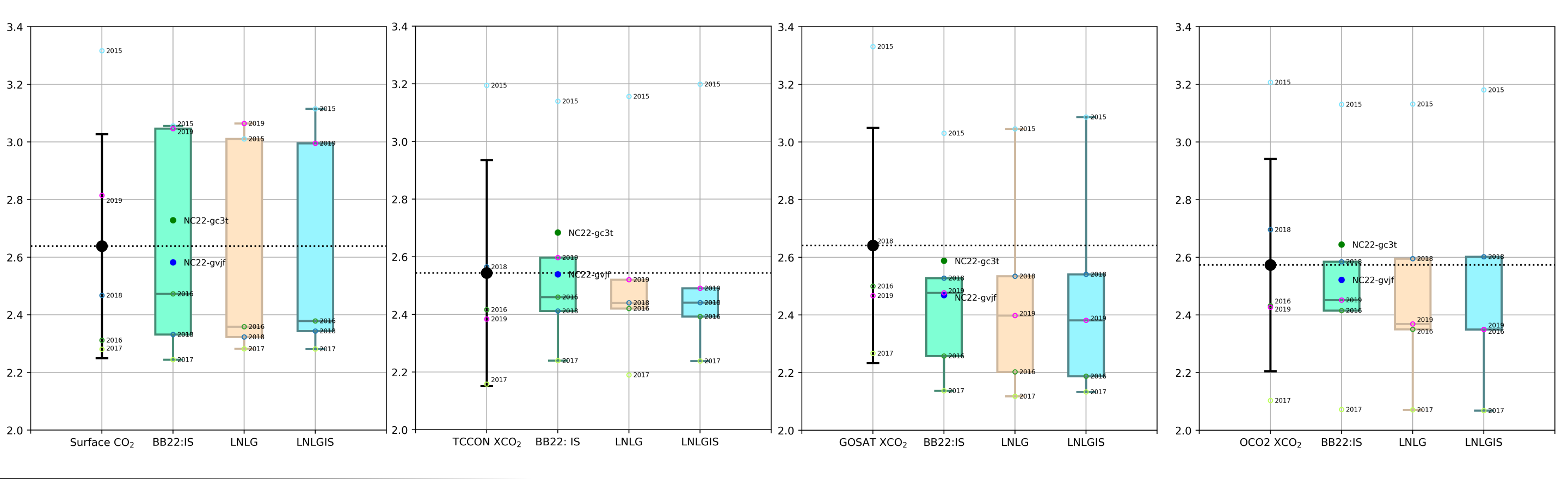
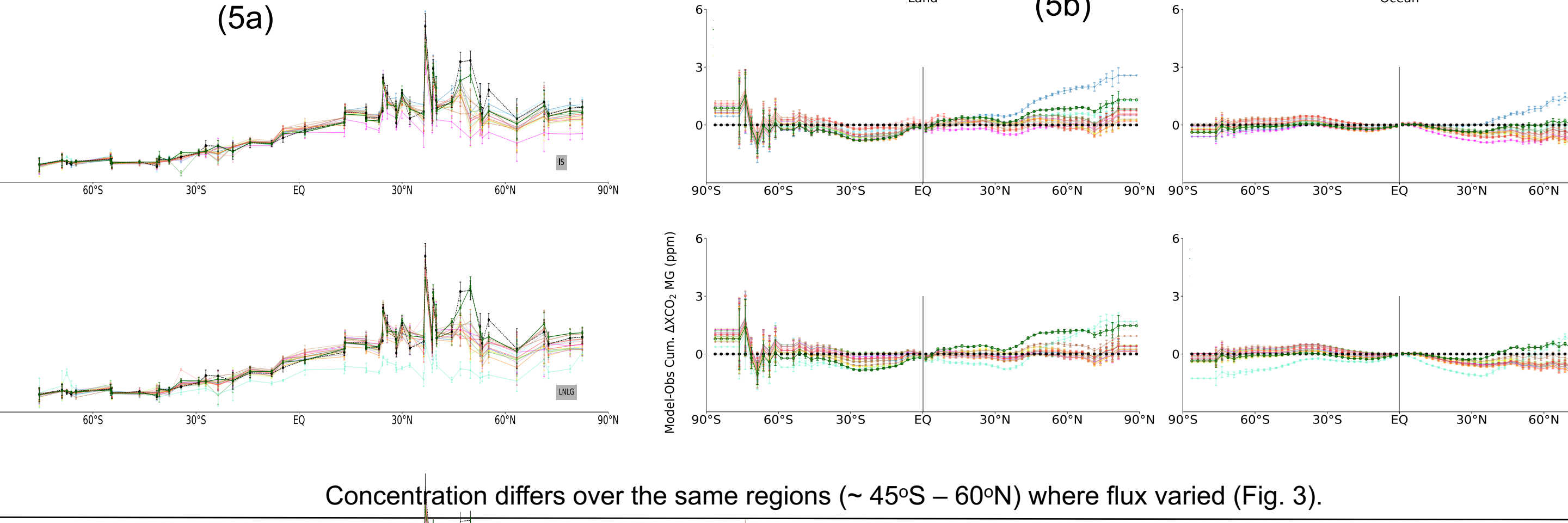
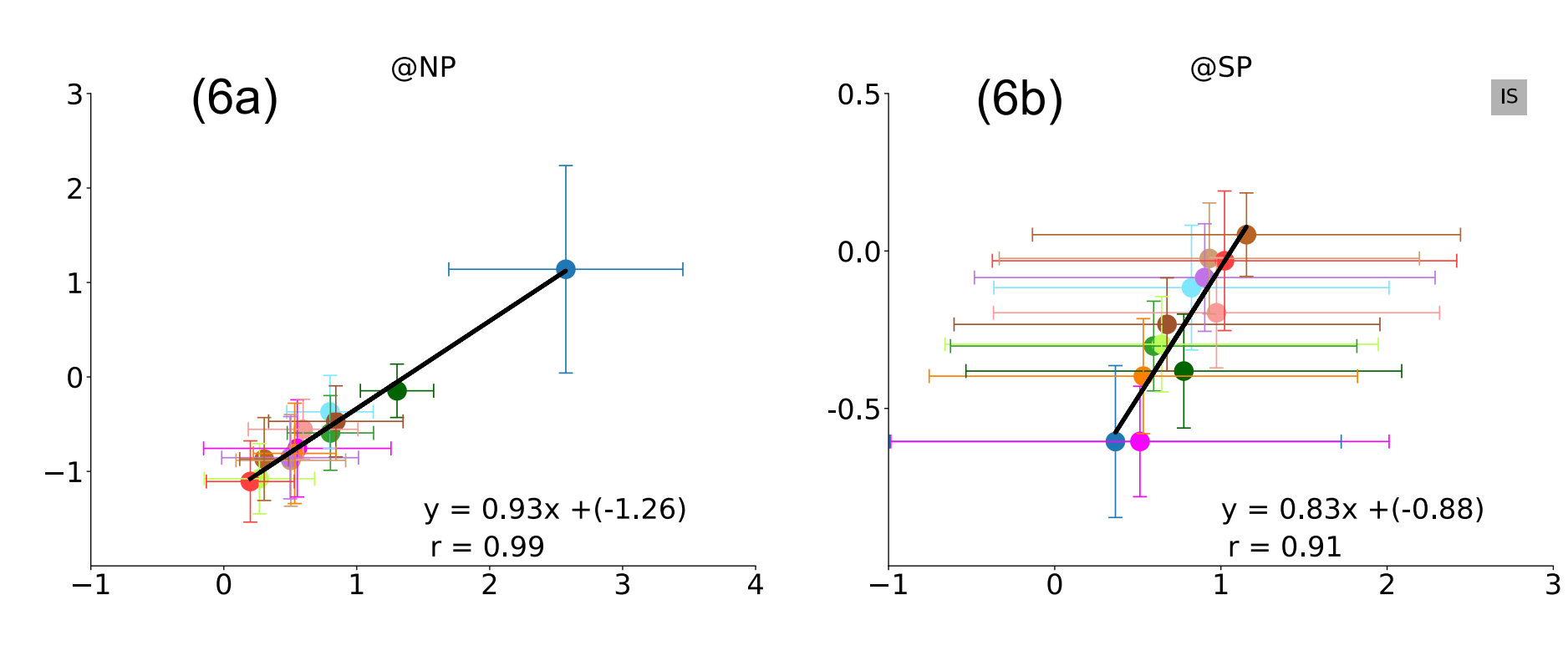


Figure 5 (below) shows meridional gradient of CO<sub>2</sub> concentration from In-situ (a) and OCO2 (b).  $\Delta\text{CO}_2/\Delta\text{XCO}_2$ =difference of concentration/columnar concentration between consecutive sites/latitude. Cumulative  $\Delta\text{CO}_2/\Delta\text{XCO}_2$  are plotted alongwith 1- $\sigma$  standard deviation (6 years period 2015 – 2020) at each sites/latitude grid.



Concentration differs over the same regions (~ 45°S – 60°N) where flux varied (Fig. 3).

Figure 6 (below) shows 2015 – 2020 average land and ocean model-observation cumulative  $\Delta\text{XCO}_2$  at NP (6a) and SP (6b) w.r.t. equator. LO, JHU and En are excluded in the calculation.

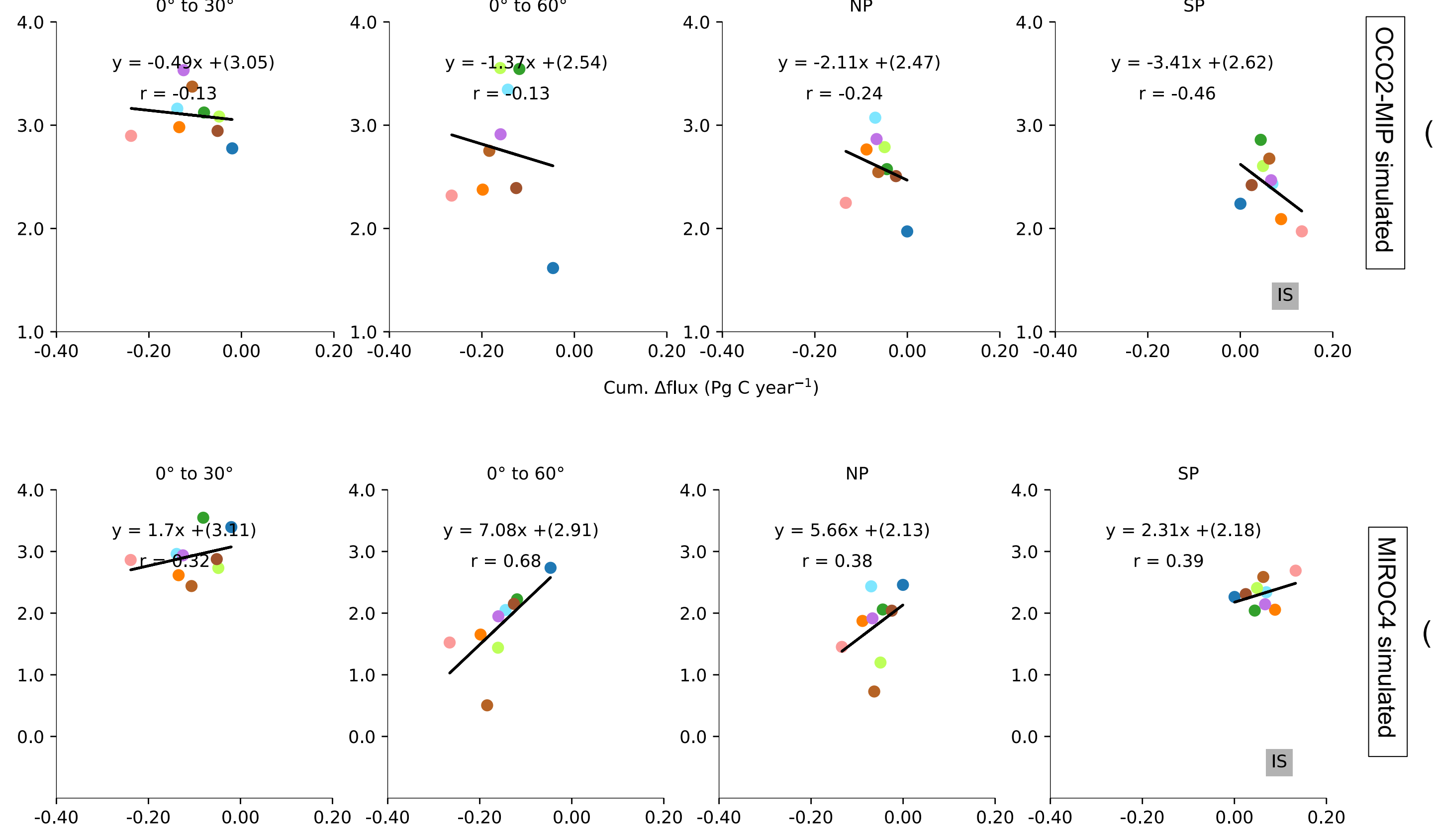


Land and ocean  $\Delta\text{XCO}_2$  gradients are strongly correlated because of fast zonal mixing of all fluxes in a given latitude band.

The source of global land-ocean flux dipole (Fig. 3) originates elsewhere, and yet to be identified.

Figure 7 (below) shows cumulative  $\Delta\text{Flux}$  vs.  $\Delta\text{CO}_2$  from in situ data (IS inversion). (7a) represents OCO2-MIP simulated and (7b) represents MIROC4 simulated. Models those are common in OCO2-MIP and MIROC4-ACTM sampled data are considered here.

OCO2-MIP fluxes simulated in a common transport model (MIROC-ACTM) show compact relationships for cumulative flux and concentration meridional gradients (7b; bottom row) compared to when the concentrations are sampled from the assimilated model fields (7a; top row).



## Conclusions

- NC22 fluxes are in good agreement with BB22 fluxes for the global land and ocean (Fig. 2), and also for the regional land and ocean fluxes except for a few land regions.
- Maximum difference in flux meridional gradients occur in the latitudes band covering productive land regions, with greater amplitude in the northern tropics to extratropics.
- As expected MIROC4-ACTM simulated growth rates are in agreement with observations from surface sites and satellites due to the constraint by global mean CO<sub>2</sub> growth rate.
- Although OCO2-MIP sampled CO<sub>2</sub> concentration gradients did not show clear dependency with the underlined flux gradients (coupled transport – flux uncertainties ??), our results using MIROC4-ACTM common transport reveal compact flux and concentration meridional gradients.

## References:

(BB22) Byrne, B., et al., National CO<sub>2</sub> budgets (2015–2020) inferred from atmospheric CO<sub>2</sub> observations in support of the Global Stocktake. *Earth System Science Data Discussions*, 1–59, 2022.

(NC22) Chandra, N., et al., Estimated regional CO<sub>2</sub> flux and uncertainty based on an ensemble of atmospheric CO<sub>2</sub> inversions. *Atmospheric Chemistry and Physics*, 22, 9215–9243, 2022.